

VARIABLES  $t$ : time  
 $x$ : zonal position  
 $y$ : meridional position  
 $\lambda$ : longitude  
 $\varphi$ : latitude  
 $a$ : the Earth radius  
 $p$ : air pressure  
 $i$ : grid number in x-direction  
 $j$ : grid number in y-direction  
 $k$ : grid number in vertical direction  
 $q$ : the amount of tracers \*  
 $u$ : zonal velocity \*  
 $v$ : meridional velocity \*  
 $F$ : the flux of tracers ( $uq$ ) \*  
 $G$ :  $uq\Delta y\Delta\sigma$  \*  
 $V$ :  $F$  when  $q = 1$  \*  
 $\Delta D$ :  $\Delta D_{j,k} = a \cos \varphi_j \Delta \lambda \Delta \varphi_j \Delta \sigma$  \*  
 $C$ : the Courant number \*  
 $I_C$ : integral fraction of the Courant number \*  
 $\hat{C}$ : decimal fraction of the Courant number \*  
 $P^S$ : Surface air pressure \*  
 $\sigma$ : normalized pressure ( $p/p^S$ ) \*  
 $\eta$ : *sigma-p* hybrid coordinate \*  
 $A$ : the coefficient for  $\eta$  coordinate \*  
 $B$ : the coefficient for  $\eta$  coordinate \*  
 \*: defined in this article

# 1 Tracer advection Scheme

## 1.1 Introduction of tracer advection scheme

MIROC6 adopts spectral method based on Spherical harmonic expansion to dynamic core. The spectral method is an excellent method, but it has some drawbacks.

1. Because of Gibbs phenomenon, noisy oscillations are produced when representing a field that is not smooth.
2. Associated with Gibbs phenomenon, negative value may occur on grids where they are not supposed to. ex.) specific humidity.
3. Global conservation of conservative quantity is good enough, but local conservation does not always hold.
4. The property that information is transmitted from upstream to downstream is not always satisfied. In spherical model, information travels instantly to the other side of the world.

Despite of these disadvantages, MIROC has adopted spectral method as dynamic core. Gibbs phenomenon usually doesn't cause any problems. However, when describing the transport of materials with strong discontinuity, the noisy oscillation and unexpected negative values sometimes appear. For example, water vapor in polar region and the stratosphere often shows discontinuous distribution because there is very small amount of water vapor. Tracers such as aerosols are also distributed locally and often show large discontinuity. These tracers are easy to be affected by Gibbs phenomenon. Therefore, in MIROC6, water vapor transport and tracer

transport are calculated using flux form semi-Lagrange (FFSL) scheme (Lin and Rood 1996) instead of using the spectral method.

Merits of this scheme are described below.

1. Gibbs phenomenon doesn't occur because it's based on gridpoint method, it enables us to represent unsmooth fields with good accuracy.
2. Negative values of tracer quantity can be avoided even in unsmooth fields.
3. No new extreme values are created.
4. Information is transmitted from upstream to downstream.
5. Conservation is satisfied locally and globally.
6. Problems which is induced by narrow grid range in polar region can be avoided.

In the next section, the principle of the tracer advection scheme is introduced in detail, and in the following section, we describe the actual implementation of the tracer advection scheme.

## 1.2 Principle of the tracer advection scheme

### 1.2.1 Transport equation in flux form

The winds and the tracer distributions are staggered in the Arakawa C-grid (Mesinger and Arakawa 1976). As example, three dimension advection equation in (x,y,p) rectangular coordinate system is given as follows.

$$\frac{\partial q}{\partial t} = -u \frac{\partial q}{\partial x} - v \frac{\partial q}{\partial y} - \omega \frac{\partial q}{\partial p} \quad (1)$$

Here,  $q$  is the amount of tracer (ex. specific humidity for water vapor),  $u, v$  is zonal and meridional velocity respectively. By substituting continuity equation to this, we get the advection equation in flux form.

$$\frac{\partial q}{\partial t} = -\frac{\partial}{\partial x}(uq) - \frac{\partial}{\partial y}(vq) - \frac{\partial}{\partial p}(\omega q) = -\frac{\partial}{\partial x}F^x - \frac{\partial}{\partial y}F^y - \frac{\partial}{\partial p}F^p \quad (2)$$

Discretizing by  $x = x_i (i = 1, 2, 3...), y = y_j (j = 1, 2, 3...), p = p_k (k = 1, 2, 3...)$ , the advection equation is rewritten as

$$\frac{\partial q_{i,j,k}}{\partial t} = \frac{1}{\Delta x_{i,j,k}}(F_{i-\frac{1}{2},j,k}^x - F_{i+\frac{1}{2},j,k}^x) + \frac{1}{\Delta y_{i,j,k}}(F_{i,j-\frac{1}{2},k}^y - F_{i,j+\frac{1}{2},k}^y) + \frac{1}{\Delta p_{i,j,k}}(F_{i,j,k-\frac{1}{2}}^p - F_{i,j,k+\frac{1}{2}}^p) \quad (3)$$

Here,  $F_{i-\frac{1}{2},j,k}^x$  is the flux in  $x$  direction at boundary between  $(i, j, k)$  and  $(i-1, j, k)$ ,  $\Delta x_{i,j,k}$  is  $x$ -direction width of grid represented as  $(i, j, k)$ . This flux formed equation automatically satisfies conservation law. The accuracy of the scheme depends on how  $F_{i-\frac{1}{2},j,k}^x$  is chosen. Next, how  $F_{i-\frac{1}{2},j,k}^x$  is determined in MIRIOC6 is explained in one dimension in  $x$ -direction, for simplicity.

### 1.2.2 The Piecewise Parabolic Method (PPM) scheme

In semi-Lagrange scheme, the flux of point  $x_{i+\frac{1}{2}}$  at time  $t$  is calculated by using  $q$  of point  $x_{i+\frac{1}{2}} - u\Delta t$  at time  $t - \Delta t$ . The value of  $u$  at time  $t$ , and  $q$  at time  $t - \Delta t$  are used. If CFL condition ( $|\frac{u\Delta t}{\Delta x}| < 1$ ) is satisfied and  $u_{i+\frac{1}{2}} > 0$ ,  $x_{i+\frac{1}{2}} - u\Delta t$  is at a point inside grid  $i$ .

As the value of  $q$  at point  $x_{i+\frac{1}{2}} - u\Delta t$ ,  $q_i$ , which is the average value of point  $i$ , can be chosen, assuming that  $q$  is constant in the grid.

However, the value of  $q$  shows large discontinuity at  $i + \frac{1}{2}$ , which is the boundary between grid  $i$  and  $i + 1$  in this assumption. This discontinuity strengthens numerical viscosity, and is unwanted for numerical

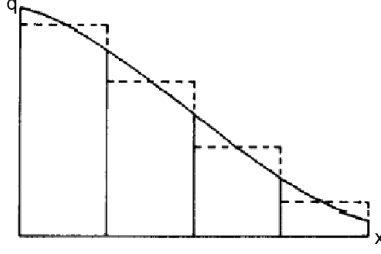


Figure 1: The image of interpolation function in PPM scheme. The interpolation function is in the solid line, the grid mean value is in the dot line.

experiments. Therefore, we want to give some kind of distribution to  $q$ , which is assumed to be constant in a grid, in order to eliminate the discontinuity and enable us to calculate  $q$  at  $x_{i+\frac{1}{2}} - u\Delta t$  by interpolation. Given distribution must be satisfied a condition as follows.

$$q_i = \frac{1}{\Delta x_i} \int_{x_{i-\frac{1}{2}}}^{x_{i+\frac{1}{2}}} q(x) dx \quad (4)$$

The old editions of MIROC adopted van Leer method, in which interpolation function is a linear function, but MIROC6 adopts The Piecewise Parabolic Method (PPM) scheme (Colella and Woodward 1984), in which interpolation function is a quadratic function (Fig.1). The FFSL scheme which adopts PPM scheme is called FFSL-3 (Lin and Rood 1996).

In PPM scheme, the distribution is determined as follows.

$$\begin{aligned} q(x) &= q_{L,i} + \xi(\Delta q_i + q_{6,i}(1 - \xi)) \\ \xi &= \frac{x - x_{i-\frac{1}{2}}}{\Delta x_i}, x_{i-\frac{1}{2}} \leq x \leq x_{i+\frac{1}{2}} \end{aligned} \quad (5)$$

Here,  $q_{L,i}$  is defined as  $\lim_{x \rightarrow x_{i+\frac{1}{2}}} q_{L,i} = q_{L,i}$ .  $q_{R,i}$  is defined as  $\lim_{x \rightarrow x_{i+\frac{1}{2}}} q_{R,i} = q_{R,i}$  as well. In PPM scheme,  $q$  is continuous at boundary  $i + \frac{1}{2}$ , therefore  $q_{L,i+1} = q_{R,i} = q_{i+\frac{1}{2}}$  is hold. In addition,

$$\Delta q_i = q_{R,i} - q_{L,i}, \quad q_{6,i} = 6(q_i - \frac{1}{2}(q_{L,i} + q_{R,i})) \quad (6)$$

For calculationg  $q_{i+\frac{1}{2}}$  by interpolation, a finite integration of  $q$  given as follows is introduced.

$$A(x) = \int_{x_{i-\frac{1}{2}}}^x q(x') dx' \quad (7)$$

At boundary of grid,

$$A(x_{i+\frac{1}{2}}) = A_{i+\frac{1}{2}} = \sum_{k \leq i} q_k \Delta x_k \quad (8)$$

$q_{i+\frac{1}{2}}$  is calculated by discretization of  $q_{i+\frac{1}{2}} = dA/dx|_{x_{i+\frac{1}{2}}}$  by using  $(A_{j+k+\frac{1}{2}}, x_{j+k+\frac{1}{2}})$ ,  $k = 0, \pm 1, \pm 2$ . Specifically,  $q_{i+\frac{1}{2}}$  is calculated as follows.

$$\begin{aligned} q_{i+\frac{1}{2}} &= q_i + \Delta x_i \frac{q_{i+1} - q_i}{\Delta x_{i+1} + \Delta x_i} + \frac{1}{\sum_{k=i-1}^{i+2} \Delta x_k} \\ &\times \left[ \frac{2\Delta x_i \Delta x_{i+1}}{\Delta x_{i+1} + \Delta x_i} \left( \frac{\Delta x_i + \Delta x_{i-1}}{\Delta x_{i+1} + 2\Delta x_i} - \frac{\Delta x_{i+2} + \Delta x_{i+1}}{2\Delta x_{i+1} + \Delta x_i} \right) (q_{i+1} - q_i) \right. \\ &\left. - \Delta x_i \frac{\Delta x_i + \Delta x_{i-1}}{\Delta x_{i+1} + 2\Delta x_i} \delta q_{i+1} + \Delta x_{i+1} \frac{\Delta x_{i+2} + \Delta x_{i+1}}{2\Delta x_{i+1} + \Delta x_i} \delta q_i \right] \end{aligned} \quad (9)$$

In case the grid width is equal in all grids, Eq.(9) can be simply rewritten as

$$q_{i+\frac{1}{2}} = \frac{1}{2}(q_{i-1} + q_i) - \frac{1}{6}(\delta q_i - \delta q_{i-1}) \quad (10)$$

Here,  $\delta q_i$  is given as

$$\delta q_i = \frac{\Delta x_i}{\Delta x_{i-1} + \Delta x_i + \Delta x_{i+1}} \left[ \frac{2\Delta x_{i-1} + \Delta x_i}{\Delta x_{i+1} + \Delta x_i} (q_{i+1} - q_i) + \frac{\Delta x_i + 2\Delta x_{i+1}}{\Delta x_{i-1} + \Delta x_i} (q_i - q_{i-1}) \right] \quad (11)$$

However, in this case, the interpolation function may have extremes in the grid and may not satisfy monotonicity. In order to avoid such a situation,  $q_{i+\frac{1}{2}}$  should be between  $q_i$  as  $q_{i+1}$ , and  $\delta q_i$  is modified as follows for that.

$$\begin{aligned} \delta_m q_i &= \min(|\delta q_i|, 2|q_i - q_{i-1}|, |q_{i+1} - q_i|) & \text{if } (q_{i+1} - q_i)(q_i - q_{i-1}) > 0, \\ &= 0 & \text{otherwise} \end{aligned} \quad (12)$$

This  $\delta q_i$  is used in Eq.(9) to calculate  $q_{i+\frac{1}{2}}$ .

When  $q(x)$  is interpolated as Eq.(5), by using Courant number defined as

$$C = \frac{u_{i+\frac{1}{2}} \Delta t}{\Delta x_{i+1}} \quad (13)$$

flux  $F_{i+\frac{1}{2}}^x$  is written as follows.

$$F_{i+\frac{1}{2}}^x = \begin{cases} u_{i+\frac{1}{2}} [q_{R,i} - \frac{C}{2}(\Delta q_i - (1 - \frac{2}{3}C)q_{6,i})] & (u_{i+\frac{1}{2}} \geq 0) \\ u_{i+\frac{1}{2}} [q_{L,i+1} + \frac{C}{2}(\Delta q_{i+1} + (1 - \frac{2}{3}C)q_{6,i+1})] & (u_{i+\frac{1}{2}} \leq 0) \end{cases} \quad (14)$$

### 1.2.3 Devices for taking long time steps

The above argument is stable only if  $C < 1$ . When the grid method is adapted to spherical coordinate,  $\Delta x$  is very small in polar region. Therefore, we have to take very small  $\Delta t$  to satisfy CFL condition. The method for avoiding  $C > 1$  and taking larger  $\Delta t$  are described below. Although this method is used for any grid widths, in this subsection we assume that  $\Delta x$  does not depend on  $i$  for simplicity.

Courant number can be divided into a integral fraction and a decimal fraction.

$$C = I_C + \hat{C}, \quad I_C : \text{aintegral fraction}, \quad -0.5 \leq \hat{C} \leq 0.5 \quad (15)$$

When  $I_C > 0$

$$F_{i-\frac{1}{2}}^x = F_{i-I_C+\frac{1}{2}}^x + \sum_{i'=i+1-I_C}^i q_{i'} \frac{\Delta x_i}{\Delta t} \quad (16)$$

When  $I_C < 0$

$$F_{i-\frac{1}{2}}^x = F_{i+|I_C|+\frac{1}{2}}^x + \sum_{i'=i+1}^{i+|I_C|} q_{i'} \frac{\Delta x_i}{\Delta t} \quad (17)$$

Where  $F_{i-I_C+\frac{1}{2}}^x$  is the flux of point  $(i - I_C + \frac{1}{2})$  calculated by using  $\hat{C}$ .

As indicated above, in the case the fluid moves in multiple grids during  $\Delta t$ , we can avoid instability of numerical calculation by evaluating the flux using the quantity  $q_{i'}$  corresponding to each grids passed. In actual, these argument is applied only to zonal flux, which can break CFL condition.

### 1.2.4 The treatment of cross terms

In the case velocity of the fluid is not only in the x-direction or y-direction, only adding the flux contributions in the x- and y-directions together underestimate the effect of diagonal advection. To take these cross term into considering, the following procedure is taken. Here, we discuss this in two-dimensional space, not in one-dimensional.

When calculating x-direction flux  $F_{i+\frac{1}{2},j}^x$ , upstream value of  $q$  in y-direction is used as value of  $q$ . That is expressed by the following equation.

$$q_{i,j}^y = \frac{1}{2}q(x_i, y_i - v_{i,j}\Delta t) + q_{i,j} \quad (18)$$

Here,  $q(x_i, y_i - v_{i,j}\Delta t)$  is calculated by linear interpolation of the two nearest grid points. In the same way, when calculating y-direction flux  $F_{i+\frac{1}{2},j}^y$ ,

$$q_{i,j}^x = \frac{1}{2}q(x_i - u_{i,j}\Delta t, y_i) + q_{i,j} \quad (19)$$

is used as  $q$ .

In the case of three dimensional tracer advection, this procedure is conducted in two dimension.

## 1.3 Actual tracer advection scheme in MIROC6

In this subsection, actual procedure of the tracer advection scheme is described. Although MIROC6 adopts  $\sigma - p$  hybrid coordinate as vertical coordinate, the tracer advection scheme is largely based on  $\sigma$  coordinate because previous version of MIROC adopted  $\sigma$  coordinate. Therefore, firstly the procedure under  $\sigma$  coordinate system is described. After this, the changes in the hybrid coordinate system from the  $\sigma$  coordinate system is described.

### 1.3.1 $\sigma$ coordinate)

The transport equation in  $\sigma$  coordinate on the sphere is expressed as

$$\frac{\partial P^S q}{\partial t} = -\frac{1}{a \cos \varphi} \frac{\partial}{\partial \lambda} (P^S u q) - \frac{1}{a \cos \varphi} \frac{\partial}{\partial \varphi} (P^S v q \cos \varphi) - \frac{\partial}{\partial \sigma} (P^S \dot{\sigma} q) \quad (20)$$

$$= \frac{1}{a \cos \varphi} \frac{\partial}{\partial \lambda} (F^\lambda) - \frac{1}{a \cos \varphi} \frac{\partial}{\partial \varphi} (F^\varphi) - \frac{\partial}{\partial \sigma} (F^\sigma) \quad (21)$$

$P^S$  is surface pressure,  $q$  is quantity of tracers. Continuity equation is given by considering the case of  $q = 1$ .

$$\frac{\partial P^S}{\partial t} = -\frac{1}{a \cos \varphi} \frac{\partial}{\partial \lambda} (P^S u) - \frac{1}{a \cos \varphi} \frac{\partial}{\partial \varphi} (P^S v \cos \varphi) - \frac{\partial}{\partial \sigma} (P^S \dot{\sigma}) \quad (22)$$

Assuming that grid is equally spaced in zonal direction, the transport equation is discretized as follows.

$$\frac{\partial P_{i,j,k}^S q_{i,j,k}}{\partial t} = \frac{1}{\Delta D_{j,k}} [(G_{i-\frac{1}{2},j,k}^\lambda - G_{i+\frac{1}{2},j,k}^\lambda) + (G_{i,j-\frac{1}{2},k}^\varphi - G_{i,j+\frac{1}{2},k}^\varphi) + (G_{i,j,k-\frac{1}{2}}^\sigma - G_{i,j,k+\frac{1}{2}}^\sigma)] \quad (23)$$

Here,

$$G_{i-\frac{1}{2},j,k}^\lambda = F_{i-\frac{1}{2},j,k}^\lambda \Delta y_j \Delta \sigma_k = (P^S u q)_{i-\frac{1}{2},j,k} \Delta y_j \Delta \sigma_k \quad (24)$$

$$G_{i,j-\frac{1}{2},k}^\varphi = F_{i,j-\frac{1}{2},k}^\varphi \Delta x_{j-\frac{1}{2}} \Delta \sigma_k = (P^S v q)_{i,j-\frac{1}{2},k} \Delta x_{j-\frac{1}{2}} \Delta \sigma_k \quad (25)$$

$$G_{i,j,k-\frac{1}{2}}^\sigma = F_{i,j,k-\frac{1}{2}}^\sigma \Delta x_j \Delta y_j = (P^S \dot{\sigma} q)_{i,j,k-\frac{1}{2}} \Delta x_j \Delta y_j \quad (26)$$

And

$$\Delta D_{j,k} = a \cos \varphi_j \Delta \lambda \Delta \varphi_j \Delta \sigma_k, \quad \Delta x_j = a \cos \varphi_j \Delta \lambda, \quad \Delta y_j = a \Delta \varphi_j \quad (27)$$

This flux form equation ensure the conservation.

For the calculation of the time-averaged mass flux across the cell boundary, the winds and the tracer distributions are staggered in the Arakawa C-grid (Mesinger and Arakawa 1976). The horizontal winds at the cell boundary,  $u_{i-\frac{1}{2},j,k}, v_{i-\frac{1}{2},j,k}$ , are reconstructed by using the mass convergence field in the spectral model and the discretized continuity equation:

$$\frac{\partial P_{i,j,k}^S}{\partial t} = \frac{1}{\Delta D_{j,k}} [(V_{i-\frac{1}{2},j,k}^\lambda - V_{i+\frac{1}{2},j,k}^\lambda) + (V_{i,j-\frac{1}{2},k}^\varphi - V_{i,j+\frac{1}{2},k}^\varphi) + (V_{i,j,k-\frac{1}{2}}^\sigma - V_{i,j,k+\frac{1}{2}}^\sigma)] \quad (28)$$

Here,  $V_{i-\frac{1}{2},j,k}^\lambda, V_{i,j-\frac{1}{2},k}^\varphi, V_{i,j,k-\frac{1}{2}}^\sigma$  denote zonal, meridional, and vertical mass-weighted wind at the cell boundary, respectively. That is,

$$V_{i-\frac{1}{2},j,k}^\lambda = (P^S u)_{i-\frac{1}{2},j,k} \Delta y_j \Delta \sigma_k \quad (29)$$

$$V_{i,j-\frac{1}{2},k}^\varphi = (P^S v)_{i,j-\frac{1}{2},k} \Delta x_j \Delta \eta_k \quad (30)$$

$$V_{i,j,k-\frac{1}{2}}^\sigma = (P^S \dot{\sigma})_{i,j,k-\frac{1}{2}} \Delta x_j \Delta y_j \quad (31)$$

$\Delta D_{j,k}$  denotes the cell volume, and  $\Delta x_j, \Delta y_j$ , and  $\Delta \sigma_k$  denote zonal, meridional and vertical width of the cell, respectively. That is  $\Delta D_{j,k} = a \cos \varphi_j \Delta \lambda \Delta \varphi_j \Delta \sigma$ ,  $\Delta x_j = a \cos \varphi_j \Delta \lambda$  and  $\Delta y_j = a \Delta \varphi_j$ .

The following are the procedure for the calculation of tracer advection in the staggering-grided horizontal and vertical wind fields:

1. Surface pressure  $P^S(t + \Delta t)$  and horizontal wind  $\mathbf{v}(\mathbf{t} + \Delta \mathbf{t})$  are predicted in the spectral model.
2. The horizontal component of mass flux divergence at time step  $t$  is calculated by using spherical harmonics. The mass fluxes at time step  $t$  are reconstructed from the values at  $t + \Delta t$  and  $t - \Delta t$  because MIROC applies semi-implicit scheme for the time-integration of surface pressure. Zonal and meridional component of mass flux divergence are:

$$C^x = -\frac{1}{a \cos \varphi} \frac{\partial}{\partial \lambda} (P^S u), \quad C^y = -\frac{1}{a \cos \varphi} \frac{\partial}{\partial \lambda} (P^S v \cos \varphi) \quad (32)$$

3. By using  $C_x$  and  $C_y$ ,  $V^\lambda, V^\varphi, V^\sigma$  are calculated as follows.

$$V_{i-\frac{1}{2},j,k}^\lambda - V_{i+\frac{1}{2},j,k}^\lambda = C_{i,j,k}^x \Delta D_{j,k}, \quad V_{i,j-\frac{1}{2},k}^\lambda - V_{i,j+\frac{1}{2},k}^\lambda = C_{i,j,k}^y \Delta D_{j,k} \quad (33)$$

The boundry conditions are  $V^\varphi = 0$  at the North Pole and South Pole,  $\sigma = 1$  at surface and  $V^\sigma = 0$  at  $\sigma = 0$ . The condition for  $V^\lambda = 0$  is:

$$\sum_i V_{i-\frac{1}{2},j,k}^\lambda = \sum_i P_{i,j,k}^S u_{i,j,k} \Delta y_j \Delta \sigma_k \quad (34)$$

That means zonal mean of zonal mass transport is equal to that in the spectral model grid. Here, the following equation must be satisfied for boundary condition  $V^\varphi = 0$  at the North Pole and the South Pole.

$$\sum_j C_{i,j,k}^y \Delta D_{j,k} = 0 \quad (35)$$

However, this is not always satisfied (On the other hand,  $\sum_i \sum_j C_{i,j,k}^y \Delta D_{j,k} = 0$  is valid within numerical error.).

In order to satisfy the boundary condition, the following correction is made.

$$C_{i,j,k}^y \leftarrow C_{i,j,k}^y - \delta C, \quad C_{i,j,k}^x \leftarrow C_{i,j,k}^x + \delta C \quad (36)$$

Here,  $\delta C = \sum_j C_{i,j,k}^y \Delta D_{j,k} / \sum_j \Delta D_{j,k}$ . Vertical velocity  $V^\eta$  is obtained by using

$$\frac{\partial P_{i,j,k}^S}{\partial t} \sum_k \Delta D_{j,k} = \sum_k (C_{i,j,k}^x + C_{i,j,k}^y) \quad (37)$$

(The contents so far are in [TRACEG]. The rest of the content is in [GTRACE])

4.  $G^\lambda, G^\varphi, G^\sigma$  are calculated by PPM scheme from  $V^\lambda, V^\varphi, V^\sigma$ .
5.  $P_{i,j,k}^s q_{i,j,k}$  at time step  $t + \Delta t$  is calculated by integration of Eq.(23) by leap frog method from  $G^\lambda, G^\varphi, G^\sigma$ .
6.  $q_{t+\Delta t}$  is calculated by dividing  $(P^s q)_{t+\Delta t}$  by  $P_{t+\Delta t}^s$ . There is small quantity of difference between  $P_{t+\Delta t}^s$  from Eq. (37) and  $P_{t+\Delta t}^s$  in the spectral model, because semi-implicit time integration scheme is applied.  $P_{t+\Delta t}^s$  from Eq. (37) is applied at present for the consistency of mass advection. Mass Conservation is not strictly satisfied because of the discrepancy between the surface pressure in the spectral model and from  $P_{t+\Delta t}^s$  Eq. (37).

### 1.3.2 $\sigma - p$ hybrid coordinate

The transport equation in  $\eta$  coordinate ( $\sigma - p$  hybrid coordinate) on the sphere is:

$$\frac{\partial m q}{\partial t} = -\frac{1}{a \cos \varphi} \frac{\partial}{\partial \lambda} (m u q) - \frac{1}{a \cos \varphi} \frac{\partial}{\partial \varphi} (m v q \cos \varphi) - \frac{\partial}{\partial \eta} (m \dot{\eta} q) \quad (38)$$

$$= \frac{1}{a \cos \varphi} \frac{\partial}{\partial \lambda} (F^\lambda) - \frac{1}{a \cos \varphi} \frac{\partial}{\partial \varphi} (F^\varphi) - \frac{\partial}{\partial \eta} (F^\eta) \quad (39)$$

Here,  $m$  corresponds to the density of the coordinate and is defined as  $m = \frac{\partial p}{\partial \eta}$ . if you look at Eq. (20), you can find that difference of  $\sigma$  coordinate and  $\eta$  coordinate is only that  $P^S$  replaces  $m$ . The actual tracer advection in  $\eta$  coordinate is mostly the same as  $\sigma$  coordinate.

In the scheme in  $\eta$  coordinate, the following variables are calculated in the same way as the way  $G^\lambda, G^\varphi, G^\eta$  is calculated in  $\sigma$  coordinate, except  $\Delta \sigma$  replaces with  $\Delta \eta$  and  $\dot{\sigma}$  replaces with  $\dot{\eta}$ .

$$G_{i-\frac{1}{2},j,k}^{\prime\lambda} = (P^S u q)_{i-\frac{1}{2},j,k} \Delta y_j \Delta \eta_k, \quad G_{i,j-\frac{1}{2},k}^{\prime\varphi} = (P^S v q)_{i,j-\frac{1}{2},k} \Delta x_{j-\frac{1}{2}} \Delta \eta_k, \quad G_{i,j,k-\frac{1}{2}}^{\prime\eta} = (P^S \dot{\eta} q)_{i,j,k-\frac{1}{2}} \Delta x_j \Delta y_j \quad (40)$$

In the time integration step, multiplying  $G'$  by  $m/P^S$ ,  $G^\lambda, G^\varphi, G^\eta$  is calculated. After that,  $m q$  at time step  $t + \Delta t$  is calculated by leap-frog method as well as  $\sigma$  coordinate.

In actual source code, combining to dividing by  $m$  to calculate  $q$  at time step  $t + \Delta t$ ,  $q$  at point  $(i, j, k)$  in time step  $t + \Delta t$  is calculated as follows.

$$\begin{aligned} q^{t+\Delta t} &= \frac{\Delta A_k + \Delta B_k P_{i,j,k}^{S,t-\Delta t}}{\Delta A_k + \Delta B_k P_{i,j,k}^{S,t+\Delta t}} q_{i,j,k}^{t-\Delta t} + \frac{2\Delta t}{\Delta D} \\ &\times [(G_{i-\frac{1}{2},j,k}^{\prime\lambda,t} - G_{i+\frac{1}{2},j,k}^{\prime\lambda,t}) + (G_{i,j-\frac{1}{2},k}^{\prime\varphi,t} - G_{i,j+\frac{1}{2},k}^{\prime\varphi,t}) + (G_{i,j,k-\frac{1}{2}}^{\prime\eta,t} - G_{i,j,k+\frac{1}{2}}^{\prime\eta,t})] \\ &\times \frac{\Delta A_k + \Delta B_k P_{i,j,k}^{S,t}}{P_{i,j,k}^{S,t}} \frac{1}{\Delta A_k + \Delta B_k P_{i,j,k}^{S,t+\Delta t}} \end{aligned} \quad (41)$$

Here,  $A, B$  is the coefficients for  $\eta$  coordinate,  $\eta_{k+\frac{1}{2}} = A_{k+\frac{1}{2}}/p_0 + B_{k+\frac{1}{2}}$  and  $\Delta A_k = A_{k-\frac{1}{2}} - A_{k+\frac{1}{2}}$ ,  $\Delta B_k = B_{k-\frac{1}{2}} - B_{k+\frac{1}{2}}$ . And  $\Delta A_k + \Delta B_k P_{i,j,k}^S = \Delta p_{i,j,k}$  (More details in the section of the vertical discretization).

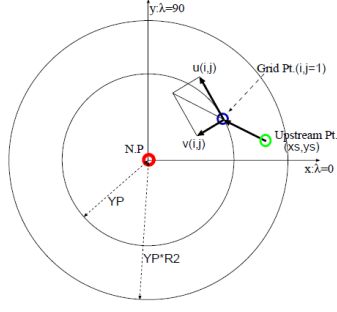


Figure 2: Conceptual figure for the flux on pole-most grids.

### 1.3.3 The mass fluxes into/out of polar caps

The mass fluxes into/out of polar caps are calculated by using the semi-Lagrangian scheme in the polar stereo projection (cf. Fig.2). The horizontal average at the highest latitude band is assumed to be preserved before/after flux calculation for the mass conservation. The sequence of calculation is:

1. Zonal average of  $P^S q$  at time step  $t$  is calculated at the highest latitude band ( $j = j_N, j_S$ ), and is assumed to equal  $P^S q$  at the pole.
2. Horizontal wind at the highest latitude bands is projected into the orthogonal coordinate system centering around the pole, and  $q$  at time step  $t + \Delta t$  is estimated by using the value at the “ departure point ”.
3. Zonal average of  $P^S q$  at time step  $t + \Delta t$  is fixed to that at  $t$ .